Obrabotka metallov (tekhnologiya, oborudovanie, instrumenty) = Metal Working and Material Science. 2024 vol. 26 no. 3 pp. 114–134
ISSN: 1994-6309 (print) / 2541-819X (online)
DOI: 10.17212/1994-6309-2024-26.3-114-134

NSTU NETI

Obrabotka metallov -
Metal Working and Material Science

Journal homepage: http://journals.nstu.ru/obrabotka_metallov

Information properties of frequency characteristics of dynamic cutting systems in the diagnosis of tool wear

Vilor Zakovorotny [a], *Valery Gvindjiliya* [b, *], *Kirill Kislov* [c]

Don State Technical University, 1 Gagarin square, Rostov-on-Don, 344000, Russian Federation

[a] https://orcid.org/0000-0003-2187-9897, vzakovorotny@dstu.edu.ru; [b] https://orcid.org/0000-0003-1066-4604, vvgvindjiliya@donstu.ru;
[c] https://orcid.org/0000-0002-5770-2519, kislovk@bk.ru

ARTICLE INFO

Article history:
Received: 22 May 2024
Revised: 14 June 2024
Accepted: 22 June 2024
Available online: 15 September 2024

Keywords:
Diagnostics of the condition of the cutting tool
Vibrations
Information models of dynamic monitoring

Funding
The study was supported by a grant within the framework of the "Nauka-2030".

ABSTRACT

Introduction. One of the directions for increasing the efficiency of cutting is related to the creation of tool wear diagnostic systems. Algorithms and devices have been developed that evaluate wear based on analysis of the vibroacoustic emission signal. These algorithms, as a rule, do not reveal the nature of its formation and the reasons for the change as wear develops. **Subject.** The paper is devoted to the analysis of the reasons for changes in vibration properties with the development of tool wear. **The aim of the work** is to study the changes in the frequency characteristics of a dynamic cutting system caused by the development of wear, and to build diagnostic information models on this basis, as well as its use in industry. **Method and methodology.** The results of mathematical simulation of a perturbed dynamic cutting system are presented, in which the observed vibration sequences are a consequence of disturbances transformed by a dynamic system, the parameters of which depend on wear. Two frequency ranges are considered. **Results and discussions.** The first range includes frequencies that lie within the bandwidth of the instrument subsystem. The second is outside of it. In the first frequency range, it has been analytically and experimentally proven that the development of wear leads to fundamental changes in the frequency properties of the cutting system as a converter of disturbances into tool vibrations. There is a shift in the natural frequencies of the oscillatory circuits formed by the cutting system, a decrease in its quality factor, and as wear develops, some identified features of the vibration spectra appear, including the ratio of the low-frequency and high-frequency parts of the spectrum, etc. In the second frequency range, a model of force emission in the form of a random pulse sequence is considered and wear is displayed in it. The results of studying the coherence function between the forces acting on the tool and vibrational displacement are presented. Information models of wear are proposed, an example of an information model of wear and the results of its use in industry are given.

For citation: Zakovorotny V.L., Gvindjiliya V.E., Kislov K.V. Information properties of frequency characteristics of dynamic cutting systems in the diagnosis of tool wear. *Obrabotka metallov (tekhnologiya, oborudovanie, instrumenty) = Metal Working and Material Science*, 2024, vol. 26, no. 3, pp. 114–134. DOI: 10.17212/1994-6309-2024-26.3-114-134. (In Russian).

Introduction

In the last forty years, in connection with the creation of automated machining systems, research has been conducted aimed at the creation of machining diagnostics systems. The problems of selecting the modes with the highest economic efficiency [1–3], minimum tool wear intensity [4, 5] are considered. Algorithms that allow evaluating the current characteristics of the state of the machine and tooling [6–9], the quality of the surface formed by cutting [10, 11] are considered. Time sequences of vibroacoustic emission (*VAE*) [7, 12–15], forces [16, 17], cutting temperature [7, 18, 19], etc. are used in the diagnostic systems. Machine vision elements, servomotor armature current [16] are also used. A special place in the creation of these systems is occupied by *VAE*. The *VAE* signal is analyzed in the frequency range (10 Hz–600 kHz), the individual subranges of which display different properties of physical and mechanical interactions in the

*** Corresponding author**
Gvindjiliya Valery E., Ph.D. (Engineering), Senior Lecturer
Don State Technical University,
1 Gagarin square,
344000, Rostov-on-Don, Russian Federation
Tel.: +7 918 583-23-33, **e-mail:** vvgvindjiliya@donstu.ru

cutting zone. In the frequency range (10–2,000) Hz the changes of macro-interactions are studied, and in the frequency range (20–600) kHz the processes of micro-contact interactions on the tool faces and in the area of primary plastic deformation are displayed. The evaluation of the state of friction nodes, including the contact between the auxiliary flank of the tool and the workpiece, is of independent importance [20, 21]. It is noted that the development of wear causes a change in the statistical properties of *VAE* in the friction node. Studies have been carried out to assess the state of machine nodes using the vibration signal during cutting [22, 23], as well as the quality of parts manufacturing [24, 25].

Special attention is paid to tool wear assessment [26–29]. Measurement transducers for vibration analysis of dynamic cutting system (*DCS*) are analyzed. Piezoelectric transducers [26, 27], laser systems [28, 29], non-contact electrical transducers such as magnetoelectric, induction, capacitive ones, etc. are considered. The construction of diagnostic systems includes methods of primary signal processing and the construction of information space in which the decisive recognition rules are considered. Typically, the *Fourier* transform [26–28] and wavelet transforms [29] of vibration sequences, auto regression spectral analysis [2, 30–33], various functionals over sequences, including algorithms for self-tuning or learning filters [34–36] are considered. The *Hilbert-Huang* transform [43] is also used. These transformations define the initial information processing. Further, neuro-fuzzy modelling algorithms [29], *Bayesian* classification rules [14, 37] are used to obtain the information model. The increase of diagnostics efficiency due to complexing of signals of different physical nature is considered [38–42]. Here, the systems of joint processing of information on forces and *VAE* [38, 39], as well as on temperature and *VAE* [40, 41] are widely spread.

In all cases, two problems are considered in the development of vibroacoustic diagnostics systems. The first problem is related to the construction of the information space, and the secondly, to the definition of the rules with the help of which it is possible to provide clustering on the basis of wear in the information space. Therefore, intuitively or experimentally, the dependence of *DCS* on wearability is analyzed. A lot of research has been devoted to the modelling of *DCS*. It is considered as a unity of subsystems interacting through cutting [44–47]. The interaction is modelled by dynamic coupling representing the dependence of forces on state coordinates [45, 46], first of all, on elastic deformations [6, 17, 24, 25]. This takes into account the regeneration of the deformation trace left on the previous turn of the workpiece [48-50], the lag of forces with respect to deformations [45, 51, 52], and the nonlinear dependence of forces on state coordinates [52–54]. The above list is far from exhausting the research in the field of *DCS*. It should be noted that these studies focus on the problem of stability, formation of attracting sets of deformations, its bifurcations, and so on. However, when solving the problems of diagnostics, it is necessary to consider *DCS* as a channel through which the information about force interactions is transmitted, in which the properties of the wear-dependent perturbation are manifested. Moreover, the properties of this channel also depend on wear, since the change in wear causes a change in the parameters of the dynamic coupling formed by cutting. There is a paper that considers the influence of parameter fluctuations on the stability of *DCS* [55]. However, the changes in these parameters are considered in quasi-statics, and its relationship with wear is not disclosed. The analysis shows that the next stage of the study of dynamic wear monitoring methods is related to the solution of two problems. Firstly, it is necessary to analyze the frequency properties of *DCS* as a channel through which information about force interactions is transmitted, for example, in the region of the auxiliary flank of the tool. Moreover, the frequency properties of this channel depend on wear. It also affects the noise immunity of the wear information transmission. Secondly, it is necessary to provide models of the power emission itself, taking into account its dependence on wear. These two problems determine the purpose of the research presented in this paper.

Research methodology

Mathematical modeling. Problem statement. Let us consider the *DCS* model, which is based on our previously obtained ideas [17, 24, 25]. In contrast to earlier studies, we will consider it perturbed by additive power noise $\mathbf{f(t)} = \{f_1, f_2, f_3\}^T$

$$m\frac{d^2X}{dt^2} + h\frac{dX}{dt} + cX = F_\Sigma(L, V, X) + f(t), \quad (1)$$

where $\boldsymbol{m} = diag(m)$, $\boldsymbol{h} = [h_{S,k}]$, $\boldsymbol{c} = [c_{S,k}]$, $\boldsymbol{s}, \boldsymbol{k} = 1,2,3$ are positively defined symmetric matrices of inertial, velocity and elastic coefficients; $\boldsymbol{X} = \{X_1, X_2, X_3\}^T \in \Re_X^{(3)}$ is a vector of tool deformations considered in the moving coordinate system of the trajectories of the machine actuating elements (*TMAE*); $F_\Sigma = F + \Phi$ is a vector-function of forces on the main *F* and auxiliary Φ flanks formed in coordinates of the *DCS* state;

$$\boldsymbol{F} = \{F_1, F_2, F_3\}^T \in \Re_X^{(3)};\ \boldsymbol{\Phi} = \{\Phi_1, \Phi_2, \Phi_3\}^T \in \Re_X^{(3)}.$$

TMAE are represented by displacements $\boldsymbol{L} = \{L_1, L_2, L_3\}^T \in \Re_L^{(3)}$ and velocities $\mathbf{d}\boldsymbol{L} / \mathbf{d}\boldsymbol{t} = \boldsymbol{V} = \{V_1, V_2, V_3\}^T \in \Re_L^{(3)}$. In addition, let us introduce the deformation velocities $\boldsymbol{V_X} = \mathbf{d}\boldsymbol{X} / \mathbf{d}\boldsymbol{t} = \{V_{X,1}, V_{X,2}, V_{X,3}\}^T \in \Re_X^{(3)}$.

Therefore, $\Re_L^{(3)}$ is the working space of the *TMAE* and the elastic deformation space $\Re_X^{(3)}$ is movable. It is defined by the trajectories ***L*** and ***V*** (fig. 1). In the following, we will rely on the motion separation method [56, 57], which allows independent consideration of "slow" motions lying within the servomotor bandwidth. It also includes displacements of the equilibrium point of elastic deformations. In real systems, the frequency range of "slow" motions is limited from above to a frequency not exceeding 10.0 Hz. This is the frequency range in which the tool tip motions are *TIEC* controlled. "Fast" motions are considered in variations relative to "slow" motions [58]. It lies within the bandwidth of the tool subsystem. This is the range between 10.0 Hz and 2.0 kHz. These motions are not controllable by *TIEC*s, but it is possible to control its properties. Fluctuations lying in this range are considered as the *VAE* of the cutting process. Let us also consider "superfast" motions lying outside the bandwidth of subsystem (**1**). Such vibrations are characterized as acoustic emission. The subsystems of "fast" and "superfast" motions are to be considered. In studying the relationship between "fast" motions and wear, the frequency response of *DCS* are considered. It changes during the development of wear. When studying "superfast" motions, the force emission signal as a random impulse sequence (*RIS*) of force actions is considered. First, let us consider the subsystem of "fast" motions. The system (**1**) has a priori specified and unchanging parameters. Therefore, the frequency characteristics of deformations "highlight" the natural frequencies of the tool subsystem. As the frequency of force perturbations in system (**1**) increases, peaks at natural frequencies and damping at antiresonances are observed. The properties of the subsystem of "fast" motions change if the forces are expressed through the state coordinates as follows [17, 24, 25]

$$T^{(0)} dF^{(0)} / dt + F^{(0)} = \rho(V_3, V_{X_3}) \left\{ t_P^{(0)} - \left[X_1 - k_p X_1(t-T) \right] \right\} \int_{t-T}^{t} \left\{ V_2(\xi) - V_{X_2}(\xi) \right\} d\xi, \tag{2}$$

where $\rho = \rho_0 \left\{ 1 + \mu \exp\left[-\varsigma (V_3 - V_{X_3}) \right] \right\}$ is a chip pressure $[\mathrm{kg/mm^2}]$; ρ_0 is a pressure in the area of low cutting speeds; μ is a dimensionless parameter; ς is a steepness factor $[\mathrm{s \cdot m^{-1}}]$; $T^{(0)}$ is a chip formation time constant $[\mathrm{s}]$; k_p is a trace regeneration coefficient, dimensionless $(0 \langle k_p \langle\langle 1)$.

Technological modes determining the *CNC* program are the following:

$$\begin{cases} t_P(t) = t_P^{(0)}(t) - \left[X_1(t) - k_p X_1(t-T) \right]; \\ S_P(t) = \int_{t-T}^{t} \left\{ V_2(\xi) - V_{X_2}(\xi) \right\} d\xi; \\ V_P(t) = Mod \left\{ \left[V_1(t) - V_{X_1}(t) \right], \left[V_2(t) - V_{X_2}(t) \right], \left[V_3(t) - V_{X_3}(t) \right] \right\}^T, \end{cases} \tag{3}$$

where $t_P(t)$, $S_P(t)$, $V_P(t)$ are depth, feed rate and cutting speed; $t_P^{(0)}(t) = R(t) - L_1(t)$.

Let us limit ourselves to longitudinal turning of a shaft of constant diameter (***D*** = const) in the following modes: $\boldsymbol{L_1(t)} = \boldsymbol{L_1(0)}$ = const, $\boldsymbol{L_2(t)} = \boldsymbol{V_1 t}$, $\boldsymbol{L_3(t)} = \boldsymbol{V_3 t}$. Turning with a tool with a plan main angle $\boldsymbol{\varphi} = \pi/2$ is considered (fig. 1). Auxiliary angle $\boldsymbol{\varphi}^1 \to 0$. Orthogonal clearance angle $\boldsymbol{\alpha} \to 0$. Usually $\boldsymbol{\alpha} < 6°$. When turning at constant modes, subject to stability of equilibrium $\boldsymbol{X} = \{X_1^*, X_2^*, X_3^*\}^T = \text{const}$, the following is true:

$$t_P^* = t_P^{(0)} - X_1^*(1 - k_p); \;\; S_P^* = V_2 T; \;\; V_P^* \approx V_3, \tag{4}$$

where $t_P^{(0)}(t) = R(t) - L_1(0)$; $X_2(t) = X_2(t - T)$ is true for equilibrium stability, so $S_P^* = V_2 T$; in (4) it is taken into account that $V_3 \rangle\rangle V_2$.

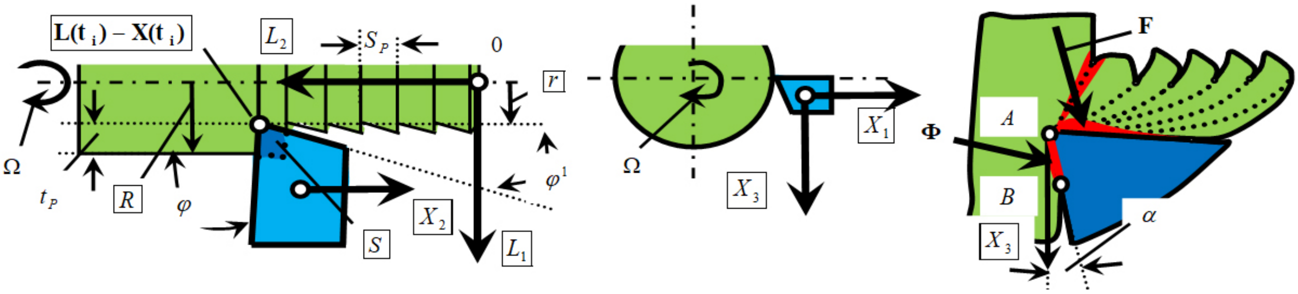

Fig. 1. Formation of forces, deformations and trajectories of actuators

Therefore, in steady state, the tool tip moves along the workpiece surface in the "***A-B***" direction. This direction is at an angle of $\boldsymbol{\varphi} = \text{arctg}(\boldsymbol{V_3}/\boldsymbol{V_2})$. The trajectory is shifted by $\boldsymbol{X}^*$ = const (fig.2). It is marked in red color. If a typical case is considered: $\boldsymbol{t_P}^{(0)} \gg \boldsymbol{S_P}^{(0)}$. Then $\boldsymbol{\Phi_1} \to 0$. For further analysis it is convenient to enter aggregated coordinates

$$\upsilon = (V_2 - dX_2 / dt) / (V_3 - dX_3 / dt) ; \;\; \upsilon^* = V_2 / V_3 . \tag{5}$$

It has been shown earlier [24, 25] that the forces $\boldsymbol{\Phi_2}$, $\boldsymbol{\Phi_3}$ are represented as

$$\begin{aligned} \Phi_2 &= k_{\hat{O}} F_0 + \rho_0 \left[t_P^{(0)} - X_1(t) \right] \exp\left[\varsigma(\upsilon - \upsilon^*) \right]; \\ \Phi_3 &= k_{\hat{O}} k_T F_0 + k_T \rho_0 \left\{ \left(t_P^{(0)} - X_1(t) \right) \exp\left[\varsigma(\upsilon - \upsilon^*) \right] \right\}, \end{aligned} \tag{6}$$

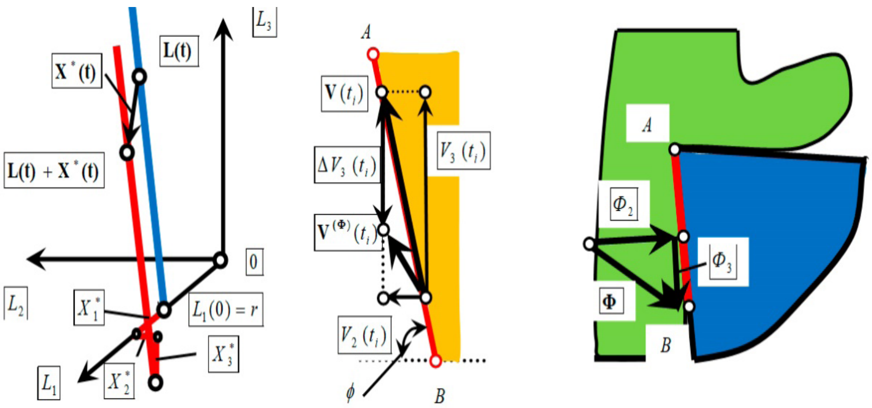

Fig. 2. Changing the direction of motion in the contact area between the rear edge of the tool and the workpiece

where ρ_0 is a force coefficient, reduced to the cutting blade contact length in [kg/mm]; ς is a parameter depending on the back angle α and tool wear; k_T is a coefficient of friction; k_Φ is a dimensionless coefficient of elastic recovery.

Equations (1)–(3) characterize the tool subsystem with nonlinear feedback. Since the system is nonlinear, its response depends on frequency and amplitude. Let us first analyze the frequency response at small perturbations.

Linearized system reactions. The linearized representation is valid for small perturbations S of the forces and variations of the shear area (Fig. 1) in the vicinity of equilibrium. Then the dynamics of the system perturbed by the forces ***f*(*t*)**, can be represented solely as a function of frequency. Moreover, it is convenient to consider the force perturbations as "white" noise. In this case, one can use the *Laplace* transform methods. For small deformations in the vicinity of equilibrium, the forces acting on the auxiliary flanks can be neglected. Then instead of (2) it is true that

$$T^{(0)}\mathrm{d}F^{(0)} / \mathrm{d}t + F^{(0)} = \bar{\rho}\left\{t_P^{(0)}S_P^{(0)} - \left[X_1 - k_p X_1(t-T)\right]S_P^{(0)} - \left[X_2(t) - X_2(t-T)\right]t_P^{(0)} + \varepsilon\right\}, \qquad (7)$$

where $\bar{\rho} = \Omega_F \int\limits_{t-(\Omega_f)^{-1}}^{t} \rho_0 \left\{1 + \mu \exp\left[-\varsigma\left(V_3 - V_{X_3}(\xi)\right)\right]\right\} d\xi \Rightarrow \rho_0\{1 + \mu\exp[-\varsigma V_3]\} = \mathrm{const}$, because $V_{X_2}(t) \to 0$; $\varepsilon = \left[X_1 - k_p X_1(t-T)\right]\left[X_2(t) - X_2(t-T)\right] = 0$, since ε is the product of small quantities.

Instead of (1) and (7) in the *Laplace* images there will be

$$\begin{cases} X_i(p) = W_{F_0 X_i}(p) F_0(p), i = 1,2,3; \\ F^{(0)} = \dfrac{\bar{\rho}\left\{t_P^{(0)}S_P^{(0)} - X_1(p)S_P^{(0)}\left[1 - k_p\exp(-Tp)\right] - X_2(p)\left[1 - \exp(-Tp)\right]t_P^{(0)}\right\}}{(1 + T^{(0)}p)}, \end{cases} \qquad (8)$$

where p is a *Laplace* image symbol; $W_{F_0,X_i}(p) = \Delta_{X_i}(p)/\Delta(p),\ i = 1,2,3$;

$$\Delta(p) = \begin{bmatrix} (mp^2 + h_{1,1}p + c_{1,1}) & (h_{2,1}p + c_{2,1}) & (h_{3,1}p + c_{3,1}) \\ (h_{1,2}p + c_{1,2},) & (mp^2 + h_{2,2}p + c_{2,2}) & (h_{3,2}p + c_{3,2},) \\ (h_{1,3}p + c_{1,3},) & (h_{2,3}p + c_{2,3},) & (mp^2 + h_{3,3}p + c_{3,3}) \end{bmatrix};$$

$$\Delta_{X_1}(p) = \begin{bmatrix} \chi_1 & (h_{2,1}p + c_{2,1}) & (h_{3,1}p + c_{3,1}) \\ \chi_2 & (mp^2 + h_{2,2}p + c_{2,2}) & (h_{3,2}p + c_{3,2},) \\ \chi_3 & (h_{2,3}p + c_{2,3},) & (mp^2 + h_{3,3}p + c_{3,3}) \end{bmatrix};$$

$$\Delta_{X_2}(p) = \begin{bmatrix} (mp^2 + h_{1,1}p + c_{1,1}) & \chi_1 & (h_{3,1}p + c_{3,1}) \\ (h_{1,2}p + c_{1,2},) & \chi_2 & (h_{3,2}p + c_{3,2},) \\ (h_{1,3}p + c_{1,3},) & \chi_3 & (mp^2 + h_{3,3}p + c_{3,3}) \end{bmatrix};$$

$$\Delta_{X_3}(p) = \begin{bmatrix} (mp^2 + h_{1,1}p + c_{1,1}) & (h_{2,1}p + c_{2,1}) & \chi_1 \\ (h_{1,2}p + c_{1,2},) & (mp^2 + h_{2,2}p + c_{2,2}) & \chi_2 \\ (h_{1,3}p + c_{1,3},) & (h_{2,3}p + c_{2,3},) & \chi_3 \end{bmatrix}.$$

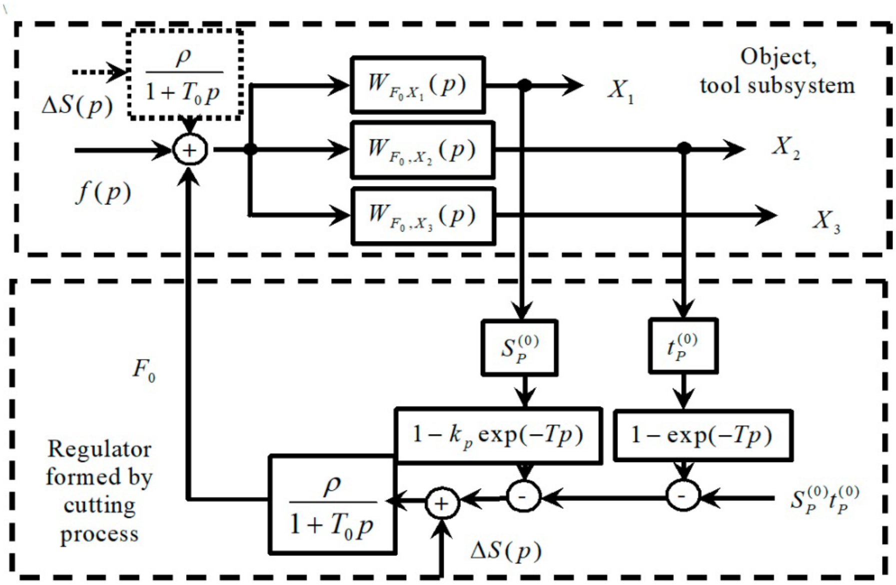

Fig. 3. Block diagram of a linearized dynamic system perturbed by forces *f (p)* and variations in the area of the cut layer *ΔS(p)*

The expressions $W_{F_0,X_i}(p) = \Delta_{X_i}(p) / \Delta(p),\ i = 1,2,3$ make sense of the dynamic compliance in the $\boldsymbol{i}$-direction. The structural diagram (fig. 3) can be put in accordance with (8). It shows that the *DCS* can be represented as an object (tool subsystem), which is covered by negative feedback (dynamic link formed by cutting). In the internal regulator, two main channels can be distinguished, which have common gain coefficients in the open state: $\boldsymbol{k_{\Sigma,1} = \rho W_{F_0 X_1}(0) S_P^{(0)}}$ and $\boldsymbol{k_{\Sigma,2} = \rho W_{F_0 X_2}(0) t_P^{(0)}}$. The effect of dynamic coupling on the frequency response depends on it. It is not difficult to see that $\boldsymbol{k_{\Sigma,2} \gg k_{\Sigma,1}}$, since $\boldsymbol{t_P{}^{(0)} \gg S_P{}^{(0)}}$.

Let us focus on the conversion of force emission $\boldsymbol{f(t)}$ into deformation displacements of the tool. To clarify other disturbances, it is sufficient to convert it to forces by adding an appropriate dynamic link. In the structural diagram (Fig. 3), the dashed line shows the conversion of the disturbance $\boldsymbol{\Delta S(t)}$ to forces. Transfer function $\boldsymbol{W_{f,X_i}(p), i} = 1,2,3$, which defines the transformation of the force emission into tool deformations is calculated using the following equation:

$$W_{f,X_i}(p) = \frac{W_{F_0,X_i}(p)}{1 + \dfrac{\rho^{(v)}}{1 + T_0 p}\left\{S_P^{(0)} W_{F_0,X_1}(p) + t_P^{(0)} W_{F_0,X_2}(p)[1 - \exp(-Tp)]\right\}}, i = 1,2,3. \quad (9)$$

Two main channels can be distinguished in the internal controller. The main one is the loop with open loop transfer function $\dfrac{\rho^{(v)}\left\{t_P^{(0)} W_{F_0,X_2}(p)[1 - \exp(-Tp)]\right\}}{1 + T_0 p}$. It follows from (9) that due to dynamic coupling, the frequency properties of the force-to-strain transformation change. The changes depend on the modes and on the parameters $\boldsymbol{\rho^{(v)}}$ and $\boldsymbol{T^{(0)}}$.

Consider the cases.

1) If $\boldsymbol{\rho^{(v)}} = 0$, then $\boldsymbol{W_{f,X_i}(p) = W_{F_0,X_i}(p)}$, and $\boldsymbol{Mod}\left\{W_{F_0,X_i}(p)\right\}$ has three resonances $\boldsymbol{\omega_{0,i}}$, $\boldsymbol{i}$ = 1, 2, 3 and two antiresonances. The effect of approximation of *DSM* frequency characteristics to the characteristics of the tool subsystem is also observed at small values of $\boldsymbol{S_P{}^{(0)}}$ and $\boldsymbol{t_P{}^{(0)}}$. Therefore, the changes in the frequency characteristics of the tool subsystem can be used to judge about the changes in the parameters of the dynamic coupling formed by cutting. At small oscillations, the main value is the parameter $\boldsymbol{\rho^{(v)}}$.

2) If $\boldsymbol{\rho}^{(v)}$ increases. Then it follows from (9) that the properties of the system change fundamentally. In particular, at resonances the amplitude bursts decrease. Moreover $\boldsymbol{\rho} < \boldsymbol{\rho}_{max}$, where $\boldsymbol{\rho}_{max}$ is the maximum permissible value at which the system is stable. The value of $\boldsymbol{\rho}_{max}$ depends on technological modes and system parameters. The value of $\boldsymbol{\rho}_{max}$ decreases with increasing the cutting depth $\boldsymbol{t_P}^{(0)}$. The value of $\boldsymbol{\rho}_{max}$ also depends on $\boldsymbol{T}^{(0)}$ and $W_{F_0 X_1}(j\omega)$.

3) If the usual turning condition $\boldsymbol{t_P}^{(0)} \gg \boldsymbol{S_P}^{(0)}$ is satisfied, the main influence on the frequency response is $\mathbf{Mod}\left\langle \frac{\rho^{(v)}}{1+T_0 j\omega}\left\{t_P^{(0)} W_{F_0,X_2}(j\omega)\left[1-\exp(-Tj\omega)\right]\right\}\right\rangle$. Then there exists such a set of frequencies $\omega \in \Delta\omega$, in which $[\mathbf{1} - \exp(-Tj\omega)]_{\omega\in\Delta\omega} = \mathbf{0}$. This is because the operator $[\mathbf{1} - \exp(-Tj\omega)]$ periodically converges to zero as the frequency increases. Therefore, the set $\boldsymbol{\omega\in\Delta\omega}$ is defined by the rotational frequency of the workpiece and multiples of it. This property leads to transformation of monotonically varying frequency characteristics to the characteristics of the comb filter type.

As a result of the study of the mathematical model, it is necessary to draw an important conclusion for further analysis: variations in the parameters of the dynamic coupling formed by cutting are reflected in changes in the frequency characteristics of the *DCS*, i.e. the channel through which information about force interactions in the cutting zone is transmitted.

Example of frequency response. Let's consider the change of *AFC* at variation $\bar{\boldsymbol{\rho}}$ and $\boldsymbol{T}^{(0)}$, for turning a shaft $\boldsymbol{R}$ = 42.0 mm made of 0.1 % *C*-1 % *Mn*-2 % *Ni*-0.5 % *Mo*-0.05 % *V* steel (*20 MnMoNi 5 5* (*DIN*), *A 508-3* (*AISI*)). The frequency response is investigated on the basis of numerical modelling in the *Matlab-Simulink* software package, as well as experimentally on the basis of direct measurement of *VAE* in the cutting process (fig. 4, 5). In modeling, a force disturbance in the form of white noise is considered. Technological modes without deformations and perturbations: feed $\boldsymbol{S_P}^{(0)}$ = 0.1 mm; depth $\boldsymbol{t_P}^{(0)}$ = 2 mm and cutting speed $\boldsymbol{V_P}^{(0)}$ = (0.5–3.8) m/s. The generalized mass is $\boldsymbol{m}$ = 0,015 kg·s^2/mm. Machining was carried out on a modernized *1K62* machine tool equipped with adjustable spindle and feed drives. Instead of a slide, a measuring system *STD.201-1* was installed to determine forces, vibration and temperature. The parameters of model are given in Table 1, Table 2.

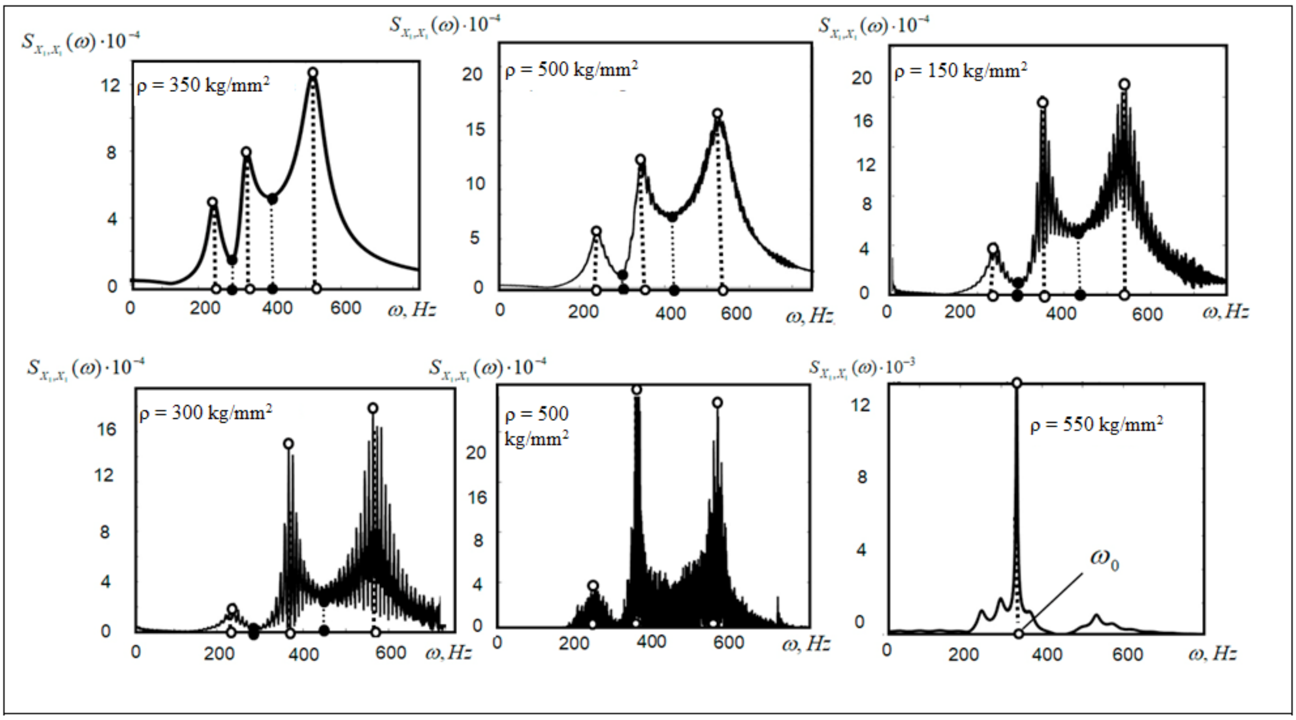

Fig. 4. Examples of changes in auto-spectra of strain depending on the pressure of chips on the leading edge of the tool

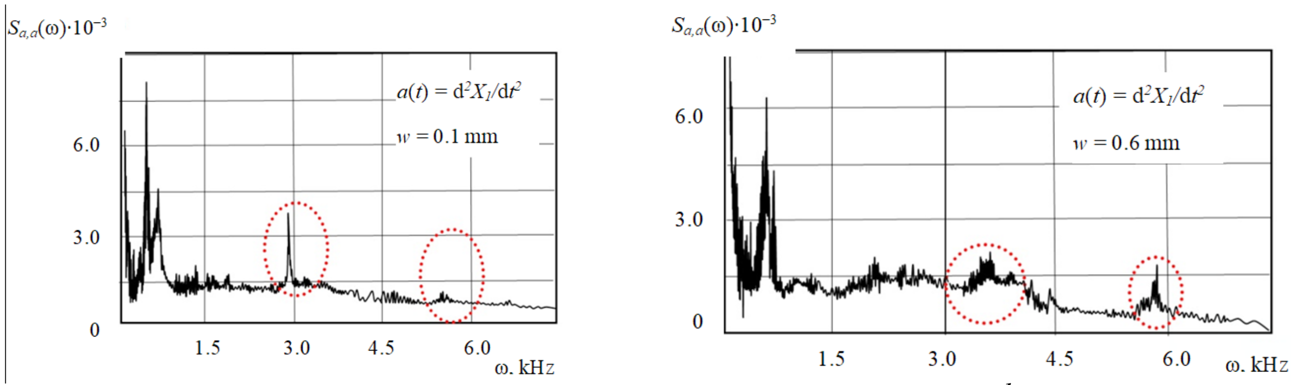

Fig. 5. An example of a *VAE* spectrum obtained from measuring vibration accelerations in the X_1 direction: *a* – wear w = 0.1 mm; *b* – wear w = 0.6 mm

Table 1

Matrices of speed coefficients and elasticity of the tool subsystem

$c_{1,1}$, kg/mm	$c_{2,2}$, kg/mm	$c_{3,3}$, kg/mm	$h_{1,1}$, kg · s/mm	$h_{2,2}$, kg · s/mm	$h_{3,3}$, kg · s/mm
4,500	1,500	750	1.3	1.1	0.8
$c_{1,2} = c_{2,1}$, kg / mm	$c_{1,3} = c_{3,1}$, kg / mm	$c_{2,3} = c_{3,2}$, kg / mm	$h_{1,2} = h_{2,1}$, kg · s / mm	$h_{1,3} = h_{3,1}$, kg · s / mm	$h_{2,3} = h_{3,2}$, kg · s / mm
200	150	80	0.6	0.5	0.4

Table 2

Dynamic link options

ρ, kg/mm^2	ρ_0, kg/mm	Ω, s^{-1}	$T^{(0)}, s$	ς	k_T	$k^{(T)}$, s/m	$k^{(S)}$	χ_1	χ_2	χ_3
100–1,000	20	5–50	0.0001	1–7	0.2	5.0	0.1	0.4	0.51	0.76

Let us consider the frequency response obtained on the basis of the calculation of auto spectrums of deformations (Fig. 4) at force perturbation in the form of “white” noise. Light round dots indicate resonances, dark dots indicate antiresonances. The following peculiarities of the frequency response change should be noted.

1. At small values of the parameter **ρ**, three bursts are noticeable in the spectrum, which correspond to the resonances of the subsystem $\boldsymbol{\omega_{0,i}}$. In between are the antiresonances. At **ρ** > (30–50) kg/mm^2, comb spectra are superimposed on the amplitude change, the distance between the bursts of which is equal to the workpiece rotation frequency of 10 Hz. Its level increases with increasing ρ. At **ρ** > 400 kg/mm^2 the spacing between bursts starts to level off and the dispersion of the spectrum increases. At **ρ** = 550 kg/mm^2 the system loses stability. It forms auto oscillations, and $\boldsymbol{S_{X,X}(\omega)}$ transforms into $\boldsymbol{\delta(\omega - \omega_0)}$-shaped spectrum with frequency $\boldsymbol{\omega_0}$ = const. At further increase of **ρ**, independent of the perturbation, different attracting sets of deformations are formed, the frequency properties of which do not depend on small perturbations. We have analyzed them in an unperturbed system earlier [17, 24, 25, 51, 52, 60].

2. The redistribution of amplitude bursts at the resonances, changes in its goodness of fit and some shift of frequencies are observed. These changes are influenced by the initial parameters. The time constant $\boldsymbol{T^{(0)}}$,

which determines the inertia of the cutting process, has a noticeable influence on the frequency response. As $\boldsymbol{T^{(0)}}$ increases, the damping of oscillations increases with frequency. Consequently, the sensitivity of frequency properties to parameter variations depends on cutting speed and plastic deformation volume. Therefore, in the high-frequency region at $\boldsymbol{\omega} \in [(\boldsymbol{T^{(0)}})^{-1}, \infty)$, the influence of the change in the dynamic coupling on the transformation of forces into deformations is cancel out.

Experimental studies of *VAE* signals measured with *Brüel & Kjær* vibration accelerometers confirm the peculiarities of the wear effect on the frequency properties of the signal, and allowed to reveal its additional features in the high-frequency region. The intensity of accelerations versus displacements in a quadratic dependence increases with increasing frequency, allowing the investigation of *VAEs* in the high-frequency region. The auto spectra are considered as Fourier images from the autocorrelation function. Therefore, the effect increases to an even greater extent.

While in the calculated spectra in fig. 4 the vibrational displacements after the resonance frequencies are practically null, the measurement of vibrational accelerations in the high-frequency region reveals bursts, which we interpret as a response to the force emission formed by cutting (highlighted by the dotted line). Let us consider the modeling of the emission.

Force emission and wear. Let us represent the power emission as a random pulse sequence [59]. It depends on two processes: periodic convergence of the auxiliary flank with the workpiece during the formation of articular and (or) elemental chips are formed (fig. 6) and on the increase in the contact area of the tool auxiliary flank and the workpiece as the tool wear develops, in which force interactions are formed. Each elementary interaction at the auxiliary flank contact site (Fig. 6), which is of molecular-mechanical nature, can be characterized by two stages. At the first stage, energy accumulation is observed (time interval $\boldsymbol{\tau}_i^{(1)}$), at the second, its release (time interval $\boldsymbol{\tau}_i^{(2)}$). The properties of an impulse can be revealed if it is represented in a triangular form. Then it will be characterised by three parameters: the distance between pulses $\boldsymbol{T}_i^{(0)}$, its duration $\boldsymbol{\tau}_i$ and height $\boldsymbol{H}_i^{(0)}$. When modelling the sequence, we can introduce hypotheses: parameters $\boldsymbol{T}_i^{(0)}$, $\boldsymbol{\tau}_i$ and $\boldsymbol{H}_i^{(0)}$ are statistically independent; its variations obey the law of normal distribution; its distribution parameters are known and they are equal. To clarify the basic properties of the signal, let us assume that its orientation in space remains unchanged and is directed by the cutting force and its modulus is equal to $\boldsymbol{f(t)}$. For such a process, its spectral representation is known [49]

$$S_{f,f}(\omega) = \frac{2\pi n}{\Delta T}\left\{(\sigma^2 + a^2)K(\omega) + 2a^2\left|H(\omega)\right|^2 \operatorname{Re}\left[\frac{\varphi(\omega)}{1-\varphi(\omega)}\right]\right\},\ i = 1,2,3\,, \tag{10}$$

where n is a number of pulses on the segment ΔT; σ is a standard deviation of amplitudes $H_i^{(0)}$; a is an expected value of $H_i^{(0)}$; $p(\tau)$ is an interval distribution function $T_i^{(0)}$; $\varphi(\omega) = \int_0^\infty e^{j\omega\tau} p(\tau) d\tau$ is a characteristic function of intervals.

Equation (10) includes $\boldsymbol{K(\omega)}$ and $\boldsymbol{H(\omega)}$, which depend on the spectrum of the standard unit pulse $K(\omega) = \int_0^\infty (\widehat{T}^{(0)})^2 \left|S(\omega, \widehat{T}^{(0)})\right|^2 p(\widehat{T}^{(0)}) d(\widehat{T}^{(0)})$, where $S(\omega, \widehat{T}^{(0)})$ is a standard pulse spectral density; $p(\widehat{T}^{(0)})$ is a probability distribution function of pulse duration; $\widehat{T}^{(0)}$ is an expected value of distances; $H(\omega) = \int_0^\infty (\hat{\tau}) S(\omega, \hat{\tau}) p(\hat{\tau}) d(\hat{\tau})$. Symbol "^" means that the mathematical expectation is considered. The functions $\boldsymbol{K(\omega)}$ and $\boldsymbol{H(\omega)}$ "paint" the spectra without changing the structure of the spectral representation. The expected values and dispersions of pulses are of main importance. The spectrum (10) is transformed by the dynamic system into the *VAE* signal, which is measurable after amplification.

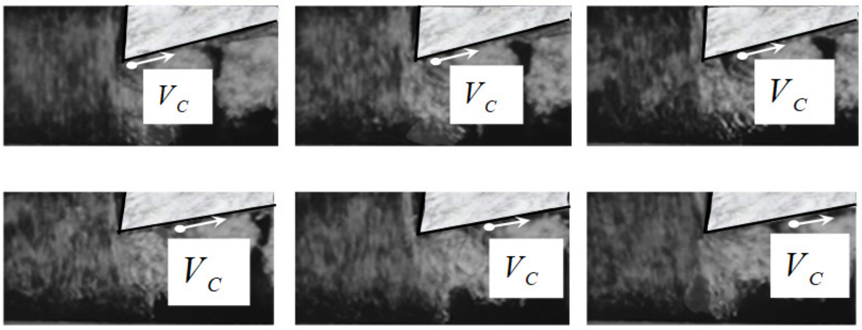

a

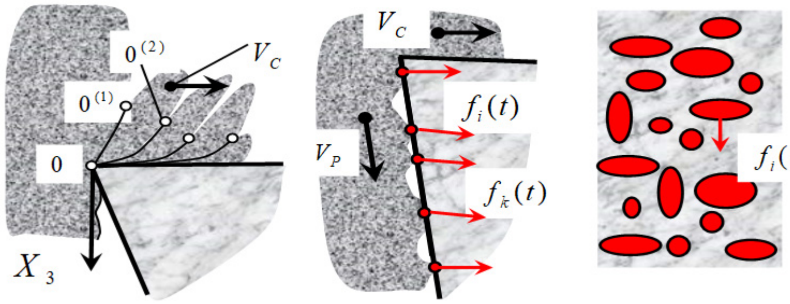

b

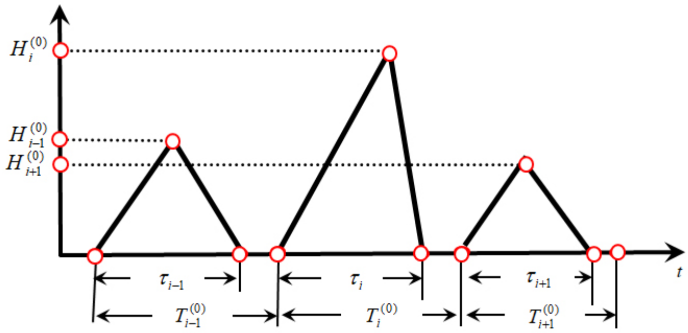

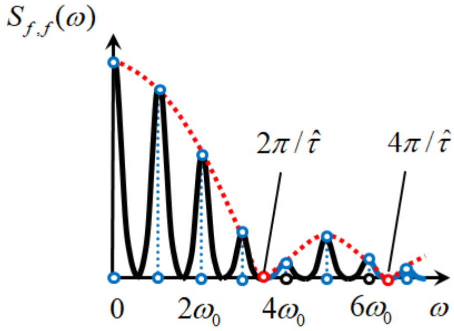

c *d*

Fig. 6. Model of force emission as a random pulse sequence:

a – fragments of high-speed filming of the formation of chip elements; *b* – diagram of the formation of fragments of power impulses; *c* – random force sequence model; *d* – example of spectral decomposition of a random sequence

It is important to note the properties of *VAE*:

– the expected value of the distances between pulses determines the burst frequency;

– the dispersion of the spacing distances causes a broadening of the spectral line (fig. 6);

– wear development causes an increase in contact interaction acts and increases the uncertainty of the pulses. Therefore, the development of wear causes a shift of the burst frequency and a broadening of its spectrum;

– the signal amplitude also indicates the development of wear. As wear increases, especially when approaching its critical value, a low-frequency amplitude modulation of the *VAE* is observed.

Fig. 7 shows examples of sequence-to-spectrum $\boldsymbol{S_{f,f}(\omega)}$ conversion. The broadening of the spectral line with increasing $\boldsymbol{\sigma_f}$ is noticeable. Its mappings in the *VAE* are also similar. The experimentally measured and given spectra in Fig. 7 qualitatively coincide, but its quantitative estimates vary depending on the technological regimes. The main frequencies of *VAE* shift to the high-frequency region as the cutting speed increases. This is due to the fact that the distances between pulses are mainly path dependent. It also depends on the current cutting area, and variations in depth and feed rate practically do not change its frequency

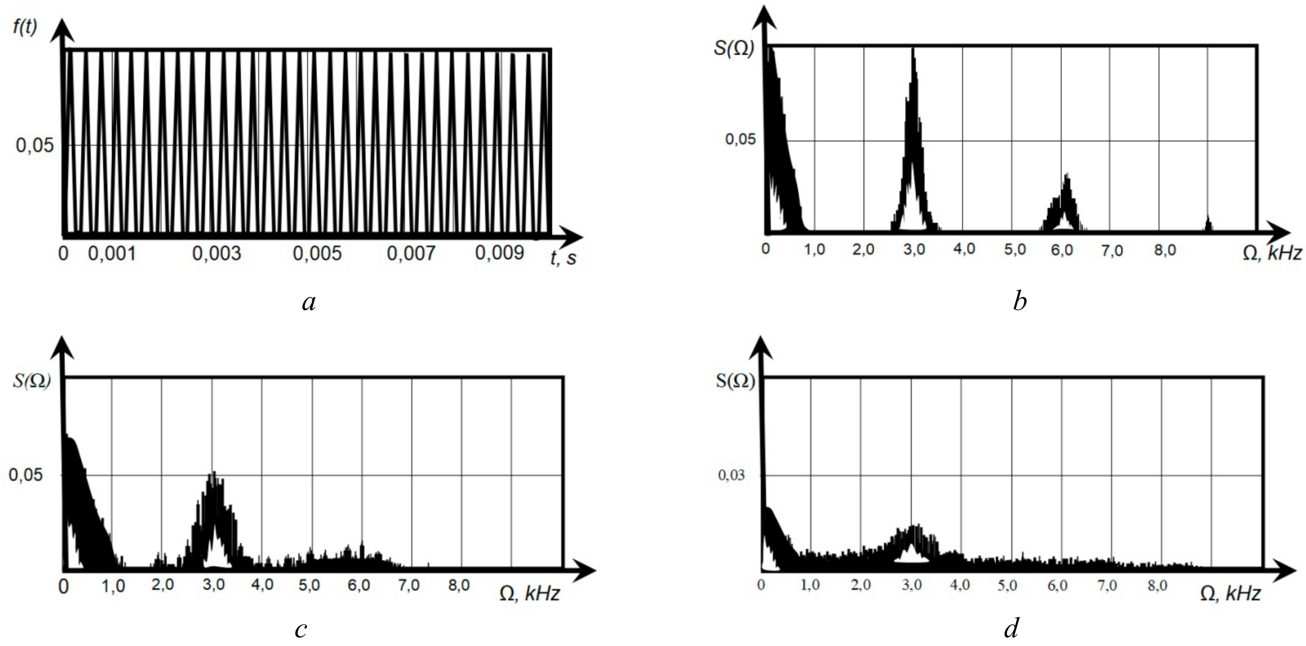

Fig. 7. Converting the pulse sequence (*a*) into its spectrum (*b*, *c*, *d*):
a – $\sigma_f = 0.01$; *b* – $\sigma_f = 0.1$; *c* – $\sigma_f = 0.2$; *d* – $\sigma_f = 0.3$

composition. In all cases there is a problem of estimating the noise immunity of the measured signal. Interferences caused by additional disturbances lie in the low-frequency region, and it can be reduced to variations of the shear area $\Delta S(t)$ [60].

The interference immunity of the signal can be estimated by the coherence function $k^2_{f,X_2}(\omega)$ between the power emission $f(t)$ and the measured sequence. To calculate $k^2_{f,X_2}(\omega)$ it is convenient to move the perturbation point of $\Delta S(t)$ to the power, as shown by the dashed line in fig. 3. Then we have

$$k^2_{f,X_2}(\omega) = \left[1 + \Delta_k(\omega)\right]^{-1}, \tag{11}$$

where $\Delta_k(\omega) = \dfrac{S_{\Delta S,\Delta S}(\omega)}{S_{f,f}(\omega)} \dfrac{\rho^2}{\left[1 + (T^0\omega)^2\right]}$; $S_{\Delta S,\Delta S}(\omega)$ is a disturbance spectrum; $S_{f,f}(\omega)$ is an emission spectrum.

The analysis of $k^2_{f,X_2}(\omega)$ shows that as the frequency increases, the conditioning of the deformation displacements by the force emission increases.

Example of vibroacoustic diagnostics. The above properties of frequency response can be used as a basis for the construction of information space. The compromise between complexity, noise immunity and informativeness, allows us to consider the following features. The first attribute takes into account the shift of the average frequency of the spectrum ω_c, determined by the rule $\int_0^{\omega_C} S(\omega)\,d\omega = \int_{\omega_C}^{\infty} S(\omega)\,d\omega$. The current value of $\omega_c(t)$ is difficult to measure. It is easier to consider the following estimation:

$$\Pi_1(w) = \left\{\int_0^{\omega_C} S_w(\omega, w)\,d\omega - \int_{\omega_C}^{\infty} S_0(\omega)\,d\omega\right\}\left\{\int_0^{\infty} S_0(\omega)\,d\omega\right\}^{-1}, \tag{12}$$

where ω_c is determined at the initial stage of wear and remains unchanged thereafter; $S_0(\omega)$ is a spectrum at the initial processing stage, when $w \to 0$; $S_w(\omega, w)$ is a wear spectrum w.

The secondly feature $\mathbf{\Pi_2(w)}$ defines the emission at the contact of the auxiliary flank of the tool. It is convenient to consider it in the form

$$\Pi_1(w) = \left\{ \int_0^{\omega_C} S_w(\omega, w)\, d\omega \int_{\omega_C}^{\infty} S_0(\omega) - d\omega \right\} \left\{ \int_0^{\infty} S_0(\omega)\, d\omega \right\}^{-1}, \tag{13}$$

where ω_c is determined at the initial stage of wear and subsequently remains unchanged; $S_0(\omega)$ is a spectrum at the initial stage of processing, when wear $w \to 0$; $S_w(\omega, w)$ is a wear spectrum.

Estimations $\mathbf{\Pi_1(w)}$ and $\mathbf{\Pi_2(w)}$ have a special feature: $\mathbf{\Pi_i(0) = 0, i = 1.2}$. The current spectrum $\mathbf{S_w(\omega,w)}$ changes as the wear progresses. Its nonstationarity $\mathbf{S_w(\omega,t)}$ in time $\mathbf{t}$ increases as $\mathbf{w}$ increases. For its estimation, let us introduce into consideration an increment of time $\mathbf{T_w}$, during which it is estimated as a movingaverage.Then,attime**t,**estimatesofthetypeofexpectation $M\{S(\omega,t)\}_{t\in[(t-T_w),t]} = \frac{1}{T_w}\int_{t-T_w}^{t} S(\omega,t)dt$ and dispersion $\sigma^2\{S(\omega,t)\}_{t\in[(t-T_w),t]} = \frac{1}{T_w}\int_{t-T_w}^{t} \{S(\omega,t) - M[S(\omega,t)]\}^2 dt$ are valid. The following estimation is informative when monotonically increasing with the development of wear:

$$\Pi_3(w) = \sigma\{S_w[\omega, w(t)]\} / M\{S_w[\omega, w(t)]\}. \tag{14}$$

The information attributes provided in the paper have the following features:

– feature $\mathbf{\Pi_1}$ characterizes a general property of the frequency response that consists in the shift of the dispersion-normalized spectrum of the *VAE* to the low-frequency region without revealing its peculiarities. For example, without revealing the shift of natural frequencies;

– features $\mathbf{\Pi_2}$ and $\mathbf{\Pi_3}$ are oriented towards analyzing the high-frequency part of the spectrum. Shortened time sequences can be used for its estimation, as these estimates are in the high-frequency part of the spectrum.

The information space is three-dimensional. The *Bayesian* rule [61] was used to determine the decisive rules for partitioning the wear into clusters. For this purpose, the clustering centers for each wear value and the dispersion of dispersion with respect to the centers were determined. Four clusters were chosen for the example: $\mathbf{w} \in (0–0.15)$ mm; $\mathbf{w} \in (0.15–0.30)$ mm; $\mathbf{w} \in (0.3–0.45)$ mm and $\mathbf{w} \in (0.45–0.60)$ mm. For each

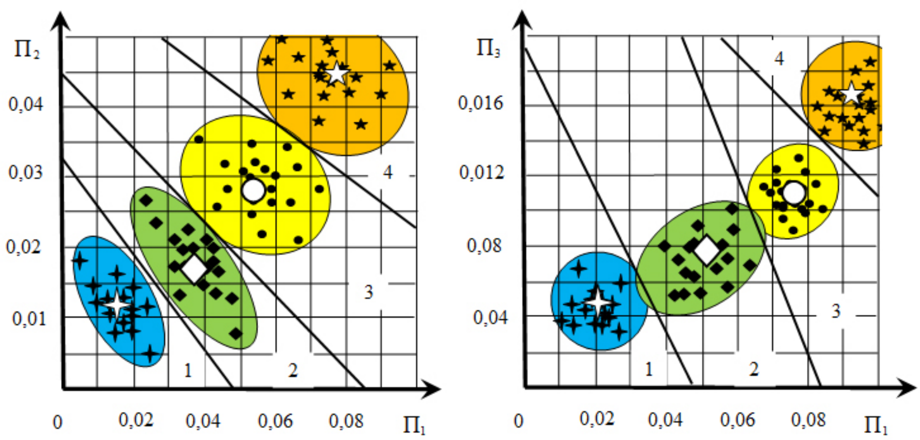

Fig. 8. Distribution of informative features in planes ($\mathbf{\Pi_1}$, $\mathbf{\Pi_2}$) and ($\mathbf{\Pi_1}$, $\mathbf{\Pi_3}$). Grouping centers are shown by shapes with a white background

cluster, dispersion ellipsoids with 95 % probability with respect to the grouping centers were determined, allowing the definition of separating hyperplanes satisfying the *Bayesian* rule. This defines the information model of diagnostics. It allows, on the basis of *VAE* measurement, to estimate the wear belonging to one of the clusters, an example of which in the planes "$\mathbf{\Pi_1}$–$\mathbf{\Pi_2}$" and "$\mathbf{\Pi_1}$–$\mathbf{\Pi_3}$" is given in fig. 8. Projections of scattering ellipses with 95 % probability and traces of hyperplanes are also given there.

The above illustrations show: if only $\mathbf{\Pi_1}$ is considered as an informative attribute, the information model can estimate only two wear classes. The given material is only an example. On the basis of the revealed peculiarities of frequency response changes in the process of wear development it is possible to build more complex information models, but not always the increase of complexity gives the increase of diagnostics accuracy. The information model is the basis for the construction of the implemented in production system of wear diagnostics on automatic lines for the production of shafts of bearing systems of combine harvesters.

Results and discussion

When building systems of dynamic diagnostics of machining processes, including tool wear, two procedures are considered. The first one includes the construction of information space. The second one considers the decisive rules that allow classification on the basis of wear. The main significance is the construction of information space. It is shown above that the development of wear changes two systems of indicators.

The development of wear causes variations in the dynamic coupling parameters, which is reflected in changes in the frequency response. It is manifested in the frequency range lying within the bandwidth of the tool subsystem. These are frequencies within the range of 100–2,000 Hz.

The cutting process is accompanied by force emission, the sources of which are associated with periodic interactions during the formation of sliding surfaces, as well as in the zone of interface between the auxiliary flanks of the tool and the workpiece. Moreover, the interactions in the area of auxiliary flank depend on its contact area, the value of which depends on wear. The frequency composition of the force emission is in the range exceeding the bandwidth of the dynamic cutting system.

These two systems, based on identifying the connection between tool wear and physical concepts of its influence on the frequency properties of *VAE*, can be used as the basis for constructing information signs for wear diagnostics. The analysis shows that the development of wear causes a change in the spectrum of *VAE*. This allows us to define the following information signs of wear display in the *VAE* signal.

The development of wear causes irreversible changes in the parameters of dynamic coupling, which cause changes in the properties of the frequency response. Among them we note the displacement of natural frequencies of subsystems, reduction of its goodness of fit, redistribution of vibration intensity in low-frequency and high-frequency regions, formation and development of periodicities in the signal spectrum, the repetition rate of which is equal to the rotation frequency of the workpiece, and so on. The development of non-stationarity of spectra as wear progresses, especially in the area of critical wear, etc., is also noted.

In the region outside the bandwidth of the tool subsystem, the development of wear causes a change in the properties of the force emission signal and its representation in deformation displacements, its velocities and accelerations. The force emission signal can be represented as a random pulse sequence. In this case, two main frequencies of the emission signal burst change, which are modelled by the force noise caused by the processes of periodic formation of sliding surfaces, as well as by periodic random interactions in the contact between the auxiliary flank of the tool and the workpiece. During the development of wear, a broadening of its spectral lines and an increase in the intensity of these signals, accompanied by its instability, are observed.

The given example of building a system of vibroacoustic diagnostics of wear in the process of machining, introduced in industry, has shown the applied efficiency of using the dependence of frequency properties of the *VAE* signal for building information models of diagnostics. The example far does not limit the possibilities of application of the regularities revealed in the paper for construction of systems of diagnostics of tool condition. To use this method for machining on *CNC* machines, it is additionally necessary to provide information exchange between the *CNC* program and the diagnostics system, since the frequency properties depend not only on wear, but also on the modes changed by the *CNC* program.

Conclusion

The aim formulated after analyzing the methods of vibroacoustic diagnostics of the cutting process has been achieved. The paper outlines theoretical provisions, mathematical models and studies aimed at elucidating the changes in the frequency characteristics of tool vibrations depending on its wear. It is shown that the frequency properties of vibration sequences measured in the cutting process change as wear develops. The research allowed us to identify two systems of indicators. **The first system** considers the frequency properties in the region including the bandwidth of subsystems interacting through cutting. In this system, the development of wear takes into account its influence on the main parameters of the dynamic coupling formed by cutting and, consequently, causes changes in the frequency properties of the signal**. The second** considers the vibrational response of the system to a power emission signal represented by a random pulse sequence.

A phenomenological model of force emission accompanying cutting in the high-frequency region outside the bandwidth of interacting subsystems is presented. It is represented as a random pulse sequence, the distribution parameters of which depend on wear. The development of wear causes an increase in the emission intensity, broadening of the spectral line of this signal, etc.

The development of wear causes changes in the parameters of the dynamic coupling formed by cutting, which causes shifts in the resonance frequencies of subsystems, a decrease in its goodness, the development of non-stationarity of spectra.

The revealed features of changes in the frequency properties of the *VAE* signal as the wear develops allows building a system of information attributes in the frequency space, which, together with the rules of clustering the information space into classes on the basis of wear, allows building an information model of wear. The given example has shown the applied efficiency of the developed methods and the given mathematical toolkit on the basis of the created and implemented in the industry system of wear diagnostics.

References

1. Ostaf'ev V.A., Antonyuk V.S., Tymchik G.S. *Diagnostika protsessa metalloobrabotki* [Diagnostics of the metalworking process]. Kiev, Tekhnika Publ., 1991. 152 p.

2. Zakovorotny V.L., Bordachev E.V., Alekseychik M.I. Dinamicheskii monitoring sostoyaniya protsessa rezaniya [Dynamic monitoring of the state of the cutting process]. *STIN*, 1998, no. 12, pp. 6–13. (In Russian).

3. Zakovorotny V., Gvindjiliya V., Process control synergetics for metal-cutting machines. *Journal of Vibroengineering*, 2022, vol. 24 (1), pp. 177–189. DOI: 10.21595/jve.2021.22087.

4. Astakhov V.P. The assessment of cutting tool wear. *International Journal of Machine Tools and Manufacture*, 2004, vol. 44, pp. 637–647. DOI: 10.1016/ j.ijmachtools.2003.11.006.

5. Konrad H., Isermann R., Oette H.U. Supervision of tool wear and surface quality during end milling operations. *IFAC Proceedings Volumes*, 1994, vol. 27 (4), pp. 507–513. DOI: 10.1016/S1474-6670(17)46074-5.

6. Zakovorotny V.L., Ladnik I.V. Postroenie informatsionnoi modeli dinamicheskoi sistemy metallorezhushchego stanka dlya diagnostiki protsessa obrabotki [Construction of an information model of the dynamic system of a metal-cutting machine for diagnostics of the machining process]. *Problemy mashinostroeniya i nadezhnosti mashin = Journal of Machinery Manufacture and Reliability*, 1991, no. 4, pp. 75–79. (In Russian).

7. Byrne G., Dornfeld D., Inasaki I., Ketteler G., Konig W., Teti R. Tool condition monitoring (TCM) – the status of research and industrial application. *CIRP Annals*, 1995, vol. 44 (2), pp. 541–567. DOI: 10.1016/S0007-8506(07)60503-4.

8. Teti R. Advanced IT methods of signal processing and decision making for zero defect manufacturing in machining. *Procedia CIRP*, 2015, vol. 28, pp. 3–15. DOI: 10.1016/ j.procir.2015.04.003.

9. Milfelner M., Cus F., Balic J. An overview of data acquisition system for cutting force measuring and optimization in milling. *Journal of Materials Processing Technology Volumes*, 2005, vol. 164–165, pp. 1281–1288. DOI: 10.1016/ j . jmatprotec.2005.02.146.

10. Kozochkin M.P., Sabirov F.S., Seleznev A.E. Vibroakusticheskii monitoring lezviinoi obrabotki zagotovok iz zakalennoi stali [Vibroacoustic monitoring of cutting edge machining of hardened steel]. *Vestnik MGTU «Stankin» = Vestnik MSUT "Stankin"*, 2018, no. 1 (44), pp. 23–30.

11. Kozochkin M.P. Mnogoparametricheskaya diagnostika tekhnologicheskikh sistem dlya obrabotki materialov rezaniem [Multivariate diagnostics of technological systems for processing materials by cutting]. *Vestnik MGTU «Stankin» = Vestnik MSUT "Stankin"*, 2014, no. 1 (28), pp. 13–19.

12. Barzov A.A., Gorelov V.A., Igonkin B.A. Akustoelektricheskaya diagnostika protsessa rezaniya polimernykh kompozitsionnykh materialov [Acoustoelectric diagnostics of the cutting process of polymer composite materials]. *Aviatsionnaya promyshlennost' = Aviation Industry*, 1986, no. 12, p. 36.

13. Bhuiyan M., Choudhury I., Nukman Y. An innovative approach to monitor the chip formation effect on tool state using acoustic emission in turning. *International Journal of Machine Tools and Manufacture*, 2012, vol. 58, pp. 19–28. DOI: 10.1016/ j.ijmachtools.2012.02.001.

14. Rehorn A.G., Jiang J., Orban P.E. State-of-the-art methods and results in tool condition monitoring: a review. *International Journal of Advanced Manufacturing Technology*, 2005, vol. 26, pp. 693–710. DOI: 10.1007/s00170-004-2038-2.

15. Jemielniak K., Arrazola P. Application of AE and cutting force signals in tool condition monitoring in micro-milling. *CIRP Journal of Manufacturing Science and Technology*, 2008, vol. 1 (2), pp. 97–102. DOI: 10.1016/ j.cirpj.2008.09.007.

16. Zakovorotny V.L., Ladnik I.V., Dhande S.G. A method for characterization of machine-tools dynamic parameters for diagnostic purposes. *Journal of Materials Processing Technology*, 1995, vol. 53 (3–4), pp. 588–600. DOI: 10.1016/0924-0136(94)01745-M.

17. Zakovorotny V.L., Flek M.B. *Dinamika protsessa rezaniya. Sinergeticheskii podkhod* [The dynamics of the cutting process. Synergistic approach]. Rostov-on-Don, Terra Publ., 2005. 880 p.

18. Astakhov V.P. *Tribology of metal catting*. Elsevier Science, 2006. 312 p. ISBN 0080466850.

19. Makarov A.D. *Optimizatsiya protsessov rezaniya* [Optimization of cutting processes]. Moscow, Mashinostroenie Publ., 1976. 278 p.

20. Kuzin V.V., Kozochkin M.P., Grigor'ev S.N., Fedorov S.Y. Chuvstvitel'nost' vibroakusticheskogo signala k izmeneniyu sostoyaniya poverkhnostnogo sloya pri trenii [Sensitivity of a vibroacoustic signal to a change in the state of the surface layer of ceramics during frictio]. *Novye ogneupory = New Refractories*, 2021, no. 5, pp. 141–146. DOI: 10.17073/1683-4518-2021-5-141-146.

21. Zakovorotny V.L., Gvindjiliya V.E. Self-organization and evolution in dynamic friction systems. *Journal of Vibroengineering*, 2021, vol. 23 (6), pp. 1418–1432. DOI: 10.21595/jve.2021.22033.

22. Kozochkin M.P. Vliyanie dinamicheskikh kharakteristik stanochnykh uzlov na vibratsii pri rezanii [The influence of the dynamic characteristics of machine components on vibrations during cutting]. *STIN*, 2014, no. 2, pp. 4–9. (In Russian).

23. Kozochkin M.P., Maslov A.R., Sabirov F.S., Porvatov A.N. *Diagnostika i sertifikatsiya metallorezhushchego oborudovaniya* [Diagnostics and certification of metal-cutting equipment]. Moscow, Innovatsionnoe mashinostroenie Publ., 2017. 240 p.

24. Zakovorotnyi V.L., Gvindjiliya V.E. Influence of speeds of forming movements on the properties of geometric topology of the part in longitudinal turning. *Journal of Manufacturing Processes*, 2024, vol. 112, pp. 202–213. DOI: 10.1016/j.jmapro.2024.01.03.

25. Zakovorotnyi V.L., Gvindjiliya V.E. Evolution of the dynamic cutting system with irreversible energy transformation in the machining zone. *Russian Engineering Research*, 2019, vol. 39 (5), pp. 423–430. DOI: 10.3103/ S1068798X19050204.

26. Lee D.E., Hwang I., Valente C.M.O., Oliveira J.F.G., Dornfeld D.A. Precision manufacturing process monitoring with acoustic emission. *International Journal of Machine Tools and Manufacture*, 2006, vol. 46 (2), pp. 176–188. DOI: 10.1016/ j.ijmachtools.2005.04.001.

27. Liu Z., Lang Z.-Q., Gui Y., Zhu Y.-P., Laalej H. Digital twin-based anomaly detection for real-time tool condition monitoring in machining. *Journal of Manufacturing Systems*, 1995, vol. 75, pp. 163–173. DOI: 10.1016/j. jmsy.2024.06.004.

28. Dimla D.E. Sensor signals for tool-wear monitoring in metal cutting operations – a review of methods. *International Journal of Machine Tools and Manufacture*, 2000, vol. 40 (8), pp. 1073–1098. DOI: 10.1016/S0890-6955(99)00122-4.

29. Choi Y., Narayanaswami R., Chandra A. Tool wear monitoring in ramp cuts in end milling using the wavelet transform. *International Journal of Advanced Manufacturing Technology*, 2004, vol. 23 (5–6), pp. 419–428. DOI: 10.1007/s00170-003-1898-1.

30. Grigoriev A.S. Instrumentarii sistemy ChPU dlya diagnostiki i prognozirovaniya iznosa rezhushchego instrumenta v real'nom vremeni pri tokarnoi obrabotke [CNC tool for diagnostic and prediction of cutting tool wear in real time for turning processing]. *Vestnik MGTU «Stankin» = Vestnik MSUT "Stankin"*, 2012, no. 1 (18), pp. 39–43.

31. Zakovorotny V.L., Bordachev E.V. Informatsionnoe obespechenie sistemy dinamicheskoi diagnostiki iznosa rezhushchego instrumenta na primere tokarnoi obrabotki [Information support for the system of dynamic diagnostics of cutting tool wear using the example of turning]. *Problemy mashinostroeniya i nadezhnosti mashin = Journal of Machinery Manufacture and Reliability*, 1995, no. 3, pp. 95–103.

32. Dolinšek S., Kopac J. Acoustic emission signals for tool wear identification. *Wear*, 1999, vol. 225, pp. 295–303.

33. Chiou R.Y., Liang S.Y. Analysis of acoustic emission in chatter vibration with tool wear effect in turning. *International Journal of Machine Tools and Manufacture*, 2000, vol. 40 (7), pp. 927–941. DOI: 10.1016/S0890-6955(99)00093-0.

34. Bhuiyan M.S.H., Choudhury I.A., Dahari M., Nukman Y., Dawal S.Z. Application of acoustic emission sensor to investigate the frequency of tool wear and plastic deformation in tool condition monitoring. *Measurement*, 2016, vol. 92, pp. 208–217. DOI: 10.1016/ j.measurement.2016.06.006.

35. Scheffer C., Kratz H., Heyns P., Klocke F. Development of a tool wear-monitoring system for hard turning. *International Journal of Machine Tools and Manufacture*, 2003, vol. 43 (10), pp. 973–985. DOI: 10.1016/S0890-6955(03)00110-X.

36. Siddhpura A., Paurobally R. A review of flank wear prediction methods for tool condition monitoring in a turning process. *International Journal of Advanced Manufacturing Technology*, 2013, vol. 65, pp. 371–393. DOI: 10.1007/s00170-012-4177-1.

37. Karandikar J., McLeay T., Turner S., Schmitz T. Tool wear monitoring using naive Bayes classifiers. *International Journal of Advanced Manufacturing Technology*, 2014, vol. 77, pp. 1613–1626. DOI: 10.1007/s00170-014-6560-6.

38. Azmi A. Monitoring of tool wear using measured machining forces and neuro-fuzzy modeling approaches during machining of GFRP composites. *Advances in Engineering Software*, 2015, vol. 82, pp. 53–64. DOI: 10.1016/ j.advengsoft.2014.12.010.

39. Kene A.P., Choudhury S.K. Analytical modeling of tool health monitoring system using multiple sensor data fusion approach in hard machining. *Measurement*, 2019, vol. 145, pp. 118–129. DOI: 10.1016/j. measurement.2019.05.062.

40. Chethan Y., Ravindra H., Krishnegowda Y. Optimization of machining parameters in turning Nimonic-75 using machine vision and acoustic emission signals by Taguchi technique. *Measurement*, 2019, vol. 144, pp. 144–154. DOI: 10.1016/j.measurement.2019.05.035.

41. Aslan A. Optimization and analysis of process parameters for flank wear, cutting forces and vibration in turning of AISI 5140: A comprehensive study. *Measurement*, 2020, vol. 163. DOI: 10.1016/j.measurement.2020.107959.

42. Mohanraj T., Shankar S., Rajasekar R., Sakthivel N., Pramanik A. Tool condition monitoring techniques in milling process – a review. *Journal of Materials Research and Technology*, 2019, vol. 9 (1), pp. 1032–1042. DOI: 10.1016/ j.jmrt.2019.10.031.

43. Kalvoda T., Hwang Y.R. A cutter tool monitoring in machining process using Hilbert–Huang transform. *International Journal of Machine Tool and Manufacture*, 2010, vol. 50 (5), pp. 495–501. DOI: 10.1016/j. ijmachtools.2010.01.006.

44. Tobias S.A., Fishwick W. Theory of regenerative machine tool chatter. *The Engineer*, 1958, vol. 205, pp. 199–203.

45. Kudinov V.A. *Dinamika stankov* [Dynamics of machine tools]. Moscow, Mashinostroenie Publ., 1967. 359 p.

46. Tlusty J., Ismail F. Basic non-linearity in machining chatter. *CIRP Annals*, 1981, vol. 30 (1), pp. 299–304. DOI: 10.1016/S0007-8506(07)60946-9.

47. Tlusty J., Polacek A., Danek C., Spacek J. *Selbsterregte Schwingungenan an Werkzeugmaschinen*. Berlin, VEB VerlagTechnik, 1962. 340 p.

48. Merritt H.E. Theory of self-excited machine-tool chatter: contribution to machine-tool chatter research – 1. *Journal of Engineering for Industry*, 1965, vol. 87 (4), pp. 447–454. DOI: 10.1115/1.3670861.

49. Hanna N.H., Tobias S. A theory of nonlinear regenerative chatter. *Journal of Engineering for Industry*, 1974, vol. 96 (1), pp. 247–255. DOI: 10.1115/1.3438305.

50. Gouskov A.M., Panovko G.Ya., Shokhin A.E. Dynamics of the rotor system of a vibrational-centrifugal separator with an elastic vibration limiter. *Journal of Machinery Manufacture and Reliability*, 2023, vol. 51 (8), pp. 733–745. DOI: 10.3103/S105261882208009X.

51. Zakovorotnyi V. Bifurcations in the dynamic system of the mechanics processing in metal-cutting tools. *WSEAS Transactions on Applied and Theoretical Mechanics*, 2015, vol. 10, pp. 102–116.

52. Zakovorotny V.L., Lukyanov A.D., Gubanova A.A., Hristoforova V.V. Bifurcation of stationary manifolds formed in the neighborhood of the equilibrium in a dynamic system of cutting. *Journal of Sound and Vibration*, 2016, vol. 368, pp. 174–190. DOI: 10.1016/j.jsv.2016.01.020.

53. Rusinek R., Wiercigroch M., Wahi P. Influence of tool flank forces on complex dynamics of a cutting process. *International Journal of Bifurcation and Chaos*, 2014, vol. 24 (9), pp. 189–201. DOI: 10.1142/S0218127414501156.

54. Rusinek R., Wiercigroch M., Wahi P. Modeling of frictional chatter in metal cutting. *International Journal of Mechanical Sciences*, 2014, vol. 89, pp. 167–176. DOI: 10.1016/j.ijmecsci.2014.08.020.

55. Zakovorotnyi V.L., Gvindjiliya V.E. Vliyanie fluktuatsii na ustoichivost' formoobrazuyushchikh traektorii pri tochenii. *Izvestiya vysshikh uchebnykh zavedenii. Severo-Kavkazskii region. Tekhnicheskie nauki = University News. North-Caucasian Region. Technical Sciences Series*, 2017, no. 2 (194), pp. 52–61.

56. Pontryagin L.S. *Izbrannye nauchnye trudy*. T. 2 [Selected works. Vol. 2]. Moscow, Nauka Publ., 1988, pp. 95–154.

57. Tikhonov A.N. Sistemy differentsial'nykh uravnenii s malymi parametrami pri starshikh proizvodnykh [Systems of differential equations with small parameters with higher derivatives]. *Matematicheskii sbornik*, 1952, vol. 31, no. 3, pp. 231–239. (In Russian).

58. Zakovorotniy V.L., Fesenko M.A., Gvindzhilia V.E. Vliyanie protsessa rezaniya na dinamicheskie svoistva privodov ispolnitel'nykh elementov stanka [Effect of the cutting process on the dynamic properties of machine actuator drives]. *Izvestiya vysshikh uchebnykh zavedenii. Mashinostroenie = BMSTU Journal of Mechanical Engineering*, 2022, no. 9, pp. 16–29. DOI: 10.18698/0536-1044-2022-9-16-29.

59. Rytov S.M. *Vvedenie v statisticheskuyu radiofiziku*. Ch. 1 [Introduction to statistical radiophysics. Pt. 1]. Moscow, Nauka Publ., 1976. 495 p.

60. Zakovorotny V.L., Gvindzhiliya V.E. Svoistva prityagivayushchikh mnozhestv deformatsionnykh smeshchenii instrumenta v traektoriyakh formoobrazuyushchikh dvizhenii pri tochenii izdelii [The properties of attracting sets of tool deformation displacements in the trajectories of the shape-generating movements in turning]. *Izvestiya vysshikh uchebnykh zavedenii. Mashinostroenie = BMSTU Journal of Mechanical Engineering*, 2022, no. 3 (744), pp. 15–30. DOI: 10.18698/0536-1044-2022-3-15-30.

61. Shlesinger M., Glavach V. *Desyat' lektsii po statisticheskomu i strukturnomu raspoznavaniyu* [Ten lectures on statistical and structural recognition]. Kiev, Naukova dumka Publ., 2004. 554 p.

Conflicts of Interest

The authors declare no conflict of interest.